Science of the Total Environment 830 (2022) 154625

Contents lists available at ScienceDirect

Science of the Total Environment

journal homepage: www.elsevier.com/locate/scitotenv

Is airborne graphene oxide a possible hazard for the sexual reproduction of wind-pollinated plants?

Davide Zanelli [a], Fabio Candotto Carniel [a,b,*], Lorenzo Fortuna [b], Elena Pavoni [c], Viviana Jehová González [d], Ester Vázquez [d,e], Maurizio Prato [b,f,g], Mauro Tretiach [a]

[a] Department of Life Sciences, University of Trieste, I-34127 Trieste, Italy
[b] Department of Chemical and Pharmaceutical Sciences, University of Trieste, I-34127 Trieste, Italy
[c] Department of Mathematics and Geosciences, University of Trieste, I-34128 Trieste, Italy
[d] Department of Organic Chemistry, Instituto Regional de Investigación Científica Aplicada (IRICA), University of Castilla-La Mancha, E-13071 Ciudad Real, Spain
[e] Department of Organic Chemistry, University of Castilla La Mancha, E-13071 Ciudad Real, Spain
[f] Center for Cooperative Research in Biomaterials (CIC biomaGUNE), Basque Research and Technology Alliance (BRTA), Paseo de Miramón 194, E-20014 Donostia, San Sebastián, Spain
[g] Basque Foundation for Science (IKERBASQUE), E-48013 Bilbao, Spain

HIGHLIGHTS

- Graphene oxide (GO) is an emerging contaminant potentially aero-dispersible.
- The sexual reproduction of anemophilous plants might be affected by airborne GO.
- We exposed flowers of four species to an atmosphere enriched in GO nanoparticles.
- Flowers intercepted GO with negative effects on pollen adhesion, not on germination.
- The effects depended mainly on the residues of the production process bound to GO.

GRAPHICAL ABSTRACT

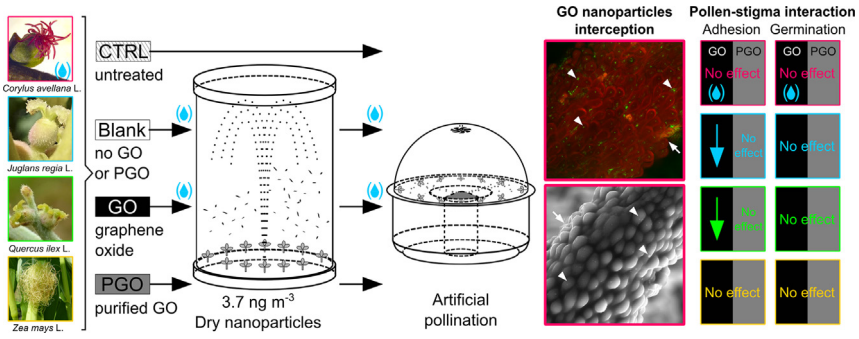

ARTICLE INFO

Article history:
Received 7 February 2022
Received in revised form 10 March 2022
Accepted 13 March 2022
Available online 16 March 2022

Editor: Elena PAOLETTI

Keywords:
Airborne nanoparticles
Graphene oxide
Anemophilous flowers
Pollen-stigma interaction

ABSTRACT

Products containing graphene-related materials (GRMs) are becoming increasingly common, allowing GRM nanoparticles (NPs) to enter the environment during their life cycle. Thanks to their lightness and bidimensional geometry, GRM NPs can be easily dispersed in the air and travel very long distances. The flowers of wind-pollinated plants may be exposed to airborne GRMs, being apt to intercept pollen from the air and, inevitably, other airborne particles. Here, stigmas of four wind-pollinated plants (*Corylus avellana*, common hazel; *Juglans regia*, walnut; *Quercus ilex*, holm oak; *Zea mays*, maize) were exposed to airborne graphene oxide (GO) and GO purified from production residues (PGO) at a concentration of 3.7 ng m^{-3}. Subsequently, the stigmas were pollinated and the adhesion of GOs and their effects on stigma integrity and pollen-stigma interaction were examined. The effect of GO NPs in presence of liquid water on the stigma of *C. avellana* was also investigated. GOs NPs were intercepted by all species, but their effect varied among them. GO reduced pollen adhesion in *J. regia* and *Q. ilex*, whereas pollen germination was unaffected in all four species. The presence of a film of water neither completely removed GO NPs from the stigma, nor it enhanced the toxic effect of GO acidity. PGO never affected pollen-stigma interaction, indicating that the phytotoxic substances used for the production of GO, still in traces in commercial GO, are the main cause of GO toxicity. These results reconfirm the need to verify GRMs effects also on key biological processes beside single model organisms.

* Corresponding author at: Department of Life Sciences, University of Trieste, I-34127 Trieste, Italy.
E-mail address: fcandotto@units.it (F. Candotto Carniel).

http://dx.doi.org/10.1016/j.scitotenv.2022.154625

1. Introduction

There are several examples in history of the introduction and use of new materials and substances, extremely useful and apparently harmless, whose negative effects on organisms and ecosystems became evident only after decades. Prominent examples are persistent organic pollutants such as dioxins, polychlorinated biphenyls, organochlorine insecticides (Miniero et al., 2015), and micro- and nanoplastics (Ivar Do Sul and Costa, 2014; Mitrano et al., 2021). The most recent breakthrough discoveries are graphene and graphene-related materials (GRMs), whose exceptional properties (Novoselov et al., 2004, 2012) have advanced many areas of research and enabled numerous practical applications (Bonaccorso et al., 2015; Shamsaei et al., 2018; Joshi et al., 2019). Even though products made with GRMs have undeniable advantages, involuntary release of GRMs nanoparticles (NPs) into the environment must be expected during their life cycle. Moreover, applications involving voluntary release of GRMs composites into the environment are currently under development (Nine et al., 2015; Liu et al., 2017; Andelkovic et al., 2018; Miraftab and Xiao, 2019; Wang et al., 2019). GRMs thus exhibit all the characteristics of emerging persistent pollutants: (*i*) increasing production volumes (Mertens, 2021), (*ii*) broad range of applications (Bonaccorso et al., 2015; Shamsaei et al., 2018; Joshi et al., 2019), (*iii*) low biodegradability (Candotto Carniel et al., 2021), and (*iv*) potentially harmful effects on organisms (Fadeel et al., 2018).

Until recently, GRMs were found in air only as by-products of combustion (also in remote Arctic regions) (Weinbruch et al., 2018), but recently they have also been detected in air from GRMs production facilities and research laboratories (Boccuni et al., 2020; Lovén et al., 2021). Indeed, GRMs have a two-dimensional (2D) geometry and an aerodynamic size smaller than their projected surface area diameter, which could lead to a longer airborne residence time (Netkueakul et al., 2020; Tombolini et al., 2021). Nevertheless, predicted environmental concentrations (PECs) for GRMs are not yet available, but they should be similar or even higher than those of other NMs such as nano-TiO_2 or ZnO (*i.e.*, approximately 1 ng m^{-3}) (Sun et al., 2014).

The effects of GRMs on organisms have been extensively studied, but their impact on ecosystems functionality is still largely unknown (Fadeel et al., 2018). Recent literature reports that sexual reproduction of seed plants, a key biological process for ecosystems, may be affected by airborne GRMs (Sun et al., 2014; Candotto Carniel et al., 2018, 2020; Zanelli et al., 2020). Among the GRMs tested, graphene oxide (GO) is the most toxic to both *in vitro* pollen performance (Candotto Carniel et al., 2018, 2020) and *in vivo* pollen-stigma interaction (Zanelli et al., 2020, 2021). However, the effects have been studied in a single model plant, the insect-pollinated (entomophilous) *Cucurbita pepo* L. (summer squash), whose flowers remain open only a few hours after blossoming (Nepi and Pacini, 1993), and are therefore at minimal risk of intercepting airborne GO. This phenomenon might occur more easily in wind-pollinated (anemophilous) plants, as the structure of their flowers maximizes interception of pollen and, indirectly, particulate matter (PM) from air. Interception of airborne GRMs would be even more likely than PM, as graphene nanoplatelets have been shown to have higher interception efficiency than spherical NaCl particles because of their longer interception length (Gao et al., 2020). Moreover, the flowers of some plants remain receptive for days or even weeks (Jones and Newell, 1948; Dupuis and Dumas, 1990; Krueger, 2000), and in exceptional cases for months. For example, *Corylus avellana* (retains the functionality of female flowers for at least two months (Germain, 1994). Therefore, GO could interact with the reproduction of anemophilous species that form the basis of human and animal nutrition (*e.g.*, cereals) and are the backbone of entire ecosystems, such as grasslands and forests.

In this work, we used microscopy techniques to verify whether GO and GO purified from its production residues (PGO) can be intercepted by the flowers of four anemophilous species with different stigmatic properties. A novel method was used to expose female flowers to an atmosphere enriched with one of the two GOs at a similar concentration to their PECs. Subsequently, the flowers were pollinated to test GO potential effects on pollen-stigma interactions. Since the toxic effects of GO are mostly observed in liquid environments (Montagner et al., 2017; Candotto Carniel et al., 2018, 2020), its interactions with the pollen-stigma system were also studied in one species in the presence of liquid water, mimicking the situation created by rain or dew.

The present work provides new insights into the interaction of GO with the flowers of anemophilous plants and the first steps of their reproduction, in order to predict and respond in time to possible negative scenarios related to the unintended release of GRMs into the atmosphere.

2. Materials and methods

2.1. GO preparation and characterization

Graphene oxide (GO; batch #GOB067) was kindly provided by Graphenea (San Sebastián, Spain) and characterized as reported by Fusco et al. (2020) and Zanelli et al. (2022, 2021). The full characterization is reported in another paper already submitted for publication (Zanelli et al., 2022) and can be found in the supplementary information (SI) appendix for completeness (SI 1). Briefly: GO elemental composition was 59.40 ± 0.10% C, 1.40 ± 0.10% H, 0.07 ± 0.02% N, and <36.6% O; the Raman spectrum of GO exhibited the characteristic bands D and G, with maxima at ~1350 and ~1600 cm^{-1}, respectively; the lateral dimension of the flakes ranged from 0.5 to 30 μm, with an average of 15.1 ± 0.4 μm, and had an average thickness of six layers (Fusco et al., 2020); a 100 μg mL^{-1} GO dispersion had a pH of 3.3 ± 0.1. Representative Raman spectra, high-resolution electron transmission microscopy images (HR-TEM) and scanning electron microscopy images (SEM) can be found in the SI Appendix (Fig. S1).

An aliquot of GO was purified from the residues of the production process ("purified GO", PGO) by washing it several times with distilled water (dH_2O) until the pH of the GO dispersion was subneutral (Ali-Boucetta et al., 2013). The supernatant removed was kept and pooled after each washing step (henceforth referred to as GO purification residue, $_{GO}$PR). Dimensional and elemental characterizations on PGO and $_{GO}$PR were performed according to Zanelli et al. (2022) and shown in Fig. S1 and Table S1, respectively. A 100 μg mL^{-1} PGO dispersion had a pH of 5.8 ± 0.3.

2.2. Plant material

Four anemophilous monoecious plants were selected on the basis of their biology and the characteristics of the stigmatic surface of the female flowers, namely *C. avellana*, *Juglans regia* L., *Quercus ilex* L. and *Zea mays* L. *C. avellana* and *J. regia* are widespread dicots that are also important from an economic point of view. *Quercus ilex* is an evergreen tree dicot typical of Mediterranean sclerophyllous vegetation, often planted in urban areas. *Zea mays* is a model monocot plant farmed worldwide.

2.2.1. Female flowers

The female inflorescences of *C. avellana* consist of eight flowers (Fig. S2a), composed of two stigma-style complexes covered by unicellular club-shaped papillae (Ciampolini and Cresti, 1998); the stigmatic surface is dry, *i.e.*, it does not secrete abundant liquid when receptive (Heslop-Harrison, 1977). The flowers of *Juglans regia* bear a large, bipartite wet stigma, *i.e.*, it is covered with a sticky fluid, characterized by several crests on its surface conferring a feathery look (Fig. S2b) (Krueger, 2000; Janković et al., 2021). The flowers of *Quercus ilex* bear a dry actinomorphic stigma with five V-shaped lobes gradually dilated at the apex and recurved (Fig. S2c); the surface extends adaxially along the stylar suture and is devoid of recognizable papillae (Gil-Pelegrín et al., 2017). *Zea mays* cobs have hundreds of silks (Fig. S2d) bearing "fibrils" (the receptive trichomes); the entire surface of each silk forms the functional dry stigma (Heslop-Harrison et al., 1984).

Female flowers were collected from 10 to 25 plants. Data on origin and time of collection are given in Table S2. Approximately two weeks before

flowering, branches of *C. avellana* and *Q. ilex* were emasculated, and female flowers were covered with paper bags to prevent uncontrolled pollination. The day before the experiments, branches or stems bearing flowers or inflorescences were cut under water and kept submerged overnight under laboratory conditions (dim light and 21 °C).

2.2.2. Pollen collection

Pollen was collected from 6 to 20 plants; information on origin and time of collection is given in Table S2. For the three dicots, branches with immature catkins were collected and immediately transported to the laboratory, where their bases were cut under water and kept immersed at laboratory conditions (see above) until flower ripening and stamen dehiscence (*ca.* 48 h). These species produce orthodox pollen that is almost completely dehydrated at stamen dehiscence but is still alive. In this state of suspended life, orthodox pollen can resist desiccation for days and is activated when rewetted over a stigmatic surface (Nepi et al., 2001). After harvest, pollen was sequentially sieved through sieves with 100 and then 60 μm mesh size to remove debris. Pollen was then dehydrated over silica gel (RH ~ 5%) for 48 h and stored at −20 °C until use. In contrast, *Z. mays* produces recalcitrant pollen which is partially hydrated and metabolically active at stamen dehiscence. Therefore, pollen dehydrates within a few hours and gradually lose its viability (Nepi et al., 2001). For this reason, the dehiscent male inflorescences of *Z. mays* were collected on the same day of the experiment between 5:00 and 6:00 a.m., transported to the laboratory, where the pollen was collected, sieved through a 500 μm mesh sieve to remove debris, and used directly for the experiments. For each species, pollen was collected in the same period as for the female flowers.

2.3. Experimental design

Female flowers were exposed to a simulated atmosphere containing a concentration of GO NPs equivalent to that predicted in the environment for other heavily produced and used NMs (Sun et al., 2016). In a first experiment, the ability of anemophilous stigmas to intercept airborne GO NPs from the air was tested using microscopy techniques. In a second experiment, the possible effect of GO and PGO NPs on pollen adhesion and germination on the stigma was tested. In a third experiment, the possible interaction of GO on the stigmatic surface of *C. avellana* in the presence of a liquid water film mimicking rain or the condensation of water vapor was checked using the same techniques.

2.4. Exposure of stigmas to airborne GO

The receptive stigmas of the target species were exposed to an atmosphere enriched in GO or PGO NPs, with all necessary measures taken to ensure workplace safety. Exposure was carried out in a custom-made 54.4 L (diam. 38 cm, H 50 cm) cylindrical deposition chamber made of polymethyl methacrylate (Ficed S.r.l., Desio, NW Italy, Fig. S3). An airbrush (AWSUC, Shenzhen Deshunke Technology Co., Ltd., Longgang, China) was placed under the chamber with the nozzle positioned in the center of the chamber bottom and vertically oriented (Fig. S3). A vent hole was placed 2 cm from the airbrush nozzle (diameter 2.5 mm) to maintain constant chamber pressure during nebulization. Air dispersions of GO and PGO NPs were obtained by nebulizing 2 mL of a 90% *v*/v ethanol/water solution enriched with GO or PGO at a concentration of 100 μg mL^{-1}. During nebulization (approximately 2 min), the vent was kept open; it was sealed after nebulization to prevent leakage of the GO NPs. Preliminary experiments were performed to find the correct setting of the airbrush (nozzle diameter: 0.3 mm; applied pressure: 1.4 bar, screw distance: 1 mm, estimated flow rate 23–25 L min^{-1}) to achieve complete liquid-gas phase transition of the nebulized ethanol/water solution and to avoid droplet condensation on the stigmatic surfaces and the walls of the chamber. An estimated concentration of 3.7 ng m^{-3} of GOs NPs was achieved in the chamber avoiding a direct flow of GO NPs on the stigmatic surface and ensuring an homogeneous vertical deposition by gravity. The air concentration of GOs NPs was only two-fold higher than the PECs of nano-ZnO (Sun et al., 2016), *i.e.* a NM produced in similar amounts as GRMs (Mertens, 2021), from 3 to 5 orders of magnitude lower than those measured in workplaces where GRMs are produced and handled (Boccuni et al., 2020; Lovén et al., 2021) and lower than the PECs of other NMs with higher production volumes, such as nano-TiO_2 (Sun et al., 2016). Therefore, the concentration used can be considered environmentally relevant.

Before each exposure of the flowers, the inner and outer surfaces of the bottom, lid and walls of the chamber were cleaned with dH_2O and dried with damp adsorbent paper to remove electrostatic charges and impurities. Small branches (~25 mm long) bearing 1 or 2 receptive flowers of *C. avellana*, *J. regia*, and *Q. ilex* were cut under water and then the base was inserted through a hole in the lid into 2-mL vials filled with water. For *Z. mays*, 25 receptive, 60-mm-long stigmatic tips were cut under water for each cob and inserted into a 2-mL vial as described above, leaving approximately 50 mm of the stigmatic surface exposed. Six to ten vials were then placed on the chamber floor, 5 cm apart and 20 cm from the nozzle (Fig. S3), and then exposed to nebulized ethanol/water GO or PGO suspension (GO/PGO samples) or ethanol/water solution (Blank samples). Blank, GO and PGO samples remained in the exposure chamber for 45 min, then the lid was removed and the samples were kept in the sealed fume hood for another 45 min under laboratory conditions to get rid of the residual ethanol. A parallel set of vials (CTRL samples) was kept under laboratory conditions (see above) and ~100% RH in a 9.2 L chamber (Kartell®, Milan, Italy) filled with 250 mL of dH_2O (humid chamber) for 1.5 h.

2.5. Adhesion of airborne GO NPs on stigmas

To verify whether GO NPs were intercepted from the air and retained by the stigmatic surface, confocal laser scanning microscopy (CLSM) and SEM in environmental mode (ESEM) were used.

CLSM in reflectance mode is one of the preferred methods for localizing GRMs in organisms and tissues (Banchi et al., 2019; Bramini et al., 2016). Stigmas from three CTRL, blank (*C. avellana* stigmas only), GO, and PGO samples were excised, mounted on glass slides with glycerin (Sigma Aldrich Chemie, Munich, Germany), and observed with a Nikon C1-si confocal microscope (Nikon, Tokyo, Japan) in reflection mode (Bramini et al., 2016). The samples were illuminated with a 514 nm laser at an intensity of 0.5%. Light reflected from GO was detected with a 525/50 bandpass filter. Stigmatic cells/papillae were visualized with a 488 nm laser (12% intensity), and their autofluorescence was detected with a 650 long-pass filter ($\lambda > 650$ nm). Five to ten fields were acquired for each sample, and 7 to 20 focal plans (stacks) were acquired for each field. Images were first processed using the denoise function of NIS Elements (version 5.21.02, Nikon, Tokyo, Japan), and then all stacks were merged into 2D images using a unification algorithm (z-projection) in ImageJ1 software (version 1.52a, NIH, Bethesda, MD, USA, 1997).

The stigmas of three CTRL, blank (*C. avellana* stigmas only), and GO specimens were excised, mounted on aluminum stubs, and observed using a Quanta250 ESEM (FEI, Oregon, USA) collecting secondary electrons (accelerating voltage: 30 kV; chamber pressure: 90 Pa). The entire stigmatic surface of each sample was examined and 10 to 15 micrographs were taken per sample. The latter were then carefully analyzed to detect structural changes in the stigma, such as agglutination/shrinkage of papillae and/or release of cytoplasmic contents, and to locate GO NPs on the surface.

2.6. Anemophilous pollination of stigmas

A specifically modified polypropylene-polycarbonate chamber (4.35 L, diam. 20 cm, H 23 cm; Kartell®, Milan, Italy) was used to disperse pollen in the air and simulate anemophilous pollination of the samples (Fig. S4). A fan of an infrared gas analyzer (IRGA) Licor 6250 (LI-COR, Lincoln, NE, USA) was connected to a BaseTech BT 153 power supply (Conrad Electronic SE, Hirschau, Germany). The fan was then attached to the top of the lid inside the chamber and oriented from top to bottom to create homogeneous air turbulence (Fig. S4). A watch glass in the middle of the chamber, below the fan, served as a support for the pollen. To prevent pollen

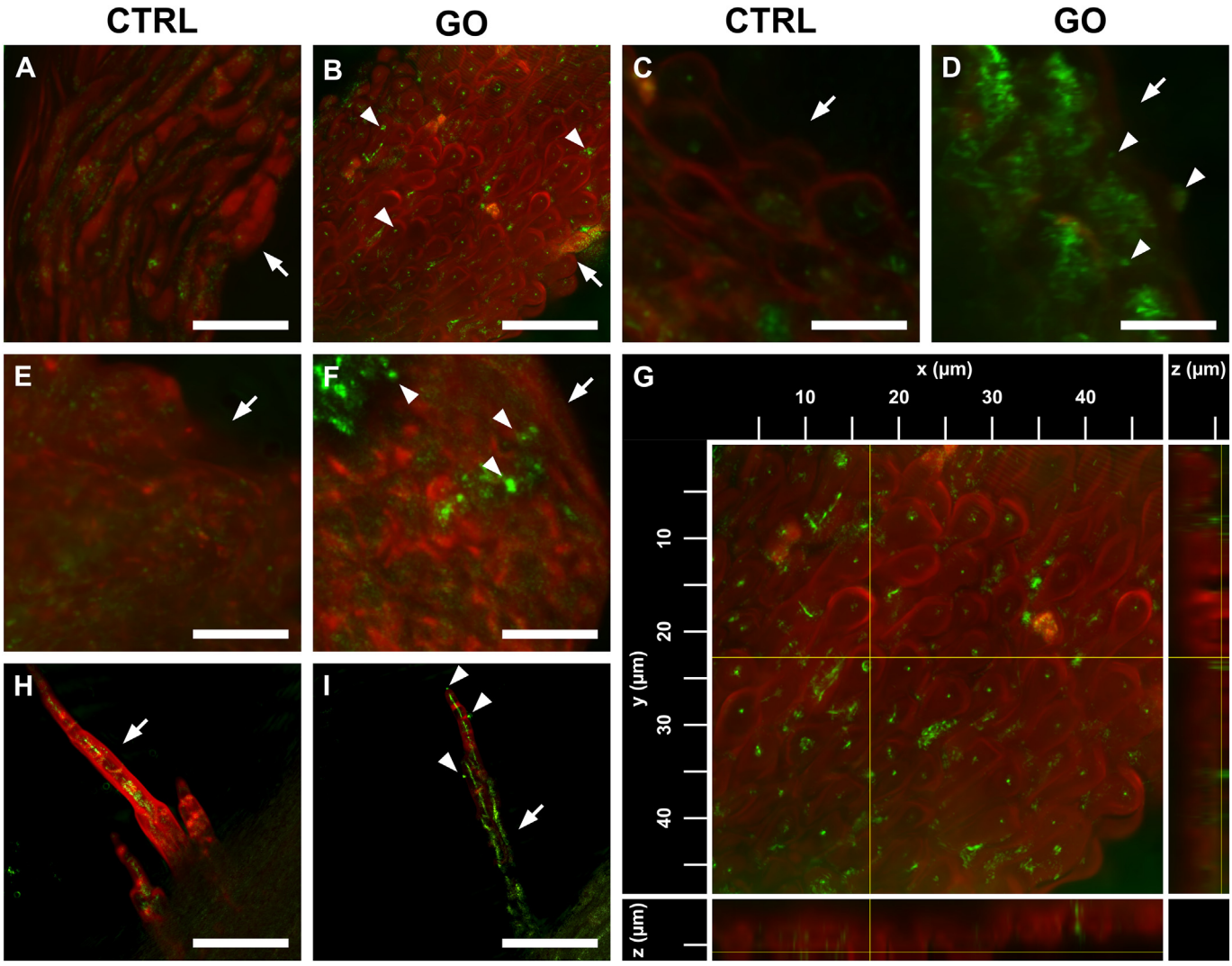

Fig. 1. Confocal laser scanning microscopy micrographs of the stigmatic surfaces of *Corylus avellana* (A, B, G), *Juglans regia* (C, D), *Quercus ilex* (E, F), and *Zea mays* (H, I) flowers observed in reflection mode. Stigmatic surfaces before (A, C, E, H) and after (B, D, F, I) exposure to airborne GO nanoparticles (for more details, see Sections 2.4, 2.5); 3D reconstruction of cells after GO exposure (G). Red signal: autofluorescence of chlorophylls; weak green signal reflected by stigmatic cells walls (A, C, E, H); strong green signal reflected by GO sheets (B, D, F, G, I). Arrows = stigmatic surface, Arrowheads = GO flakes, Bars = 100 μm.

from escaping the chamber during operation, a double foam rubber seal was placed between the lid and the bottom edges. Dispersion of pollen by air turbulence was achieved by setting the power supply to 15.8 V. The viability of pollen used for simulated anemophilous pollination was always assessed before each exposure using the fluorescein diacetate (Sigma Aldrich, Munich, D) fluorochromatic reaction, with at least 200 pollens counted (Heslop-Harrison and Heslop-Harrison, 1970). Pollen viability was greater than 80% for *C. avellana* and *Z. mays* and greater than 50% for *J. regia* and *Q. ilex*. Anemophilous pollination was performed by (*i*) placing randomly selected CTRL, Blank, GO and PGO samples (n = 4–10) on the inner rim of the chamber, (*ii*) placing an aliquot of pollen (7.5 mg for *C. avellana*, *J. regia* and *Q. ilex* and 20 mg for *Z. mays*) in the center of the watch glass and then (*iii*) activating the fan for 15 s to disperse the pollen in the air and pollinate the stigmatic surfaces. Then the samples were turned upside down and pollination was repeated to achieve homogeneous pollination. The pollen was then allowed to germinate on the stigmas overnight under laboratory conditions (see above) in a humid chamber.

2.7. Pollen adhesion and germination on the stigmatic surface

Pollen adhesion and germination on the stigmatic surface were assessed using the aniline blue staining protocol described in Zanelli et al. (2020), with reagent volumes adjusted to the size of the stigmas of the species tested: 250, 400, 350, and 2500 μL of NaOH 8 N and dH_2O were used for *C. avellana*, *J. regia*, *Q. ilex*, and *Z. mays*, respectively. Pollen adhesion was estimated by counting the total number of pollen grains detached from the stigmatic surface (n = 4–10) and expressed as a percentage difference from the CTRL samples. Germination rate was calculated as the percentage of germinated pollen grains still adhering to the stigma (n = 4–8) by counting 131 ± 64 pollen grains per stigma.

Fig. 2. SEM micrographs of stigmas of *Corylus avellana* (A, B), *Juglans regia* (C, D), *Quercus ilex* (E, F), and *Zea mays* (G, H) flowers observed in environmental mode. Stigmatic surfaces before (A, C, E, G) and after (B, D, F, H) exposure to airborne GO nanoparticles (NPs) (for more details, see Sections 2.4, 2.5); Arrows = stigmatic surface, Arrowheads = GO NPs, Bars = 50 μm.

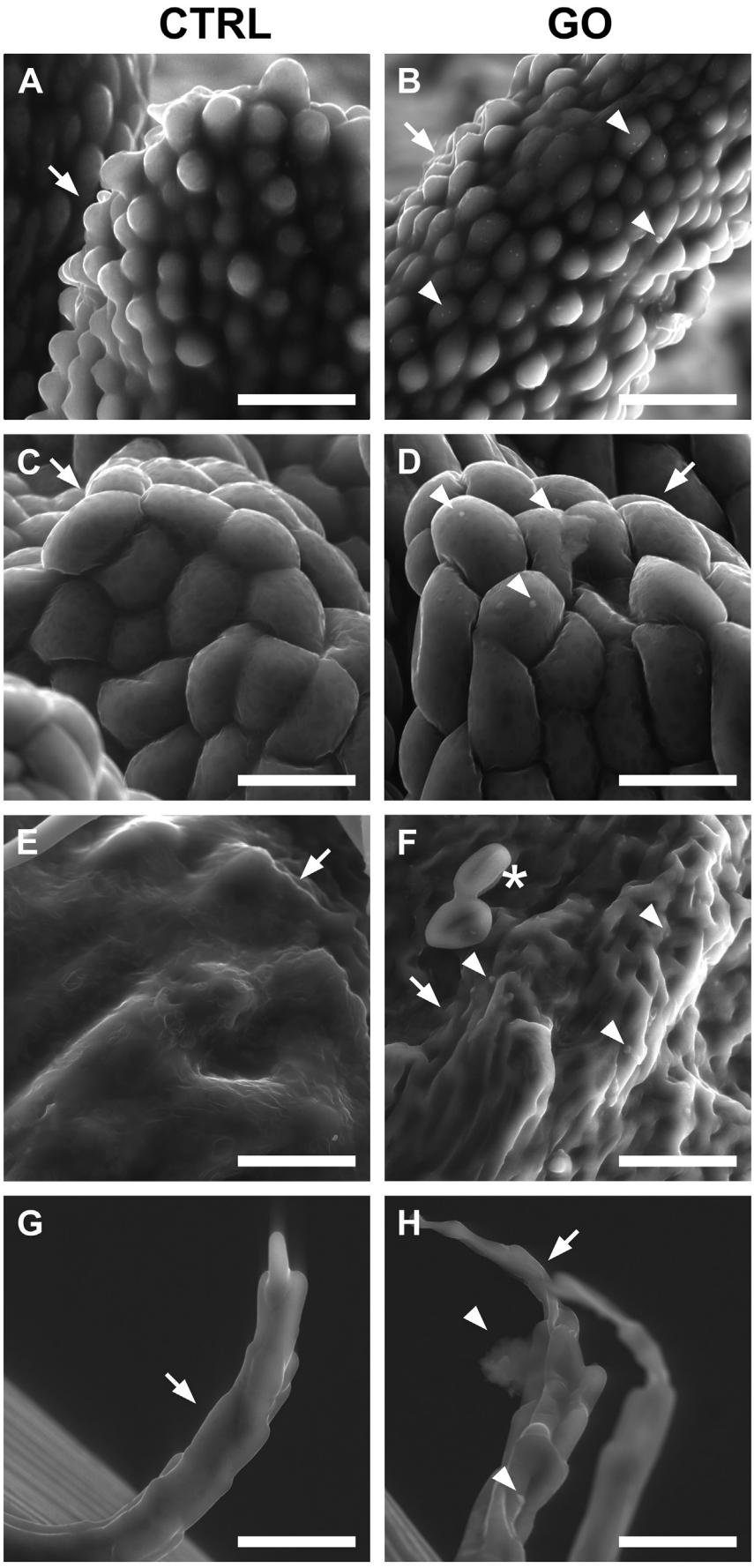
CTRL
GO
A
B
C
D
E
F
G
H

2.8. GO interaction with films of liquid water

The toxic effects of GO have been mostly observed in liquid environment (Montagner et al., 2017; Fadeel et al., 2018; Candotto Carniel et al., 2018, 2020), thus we verified if the presence of films of liquid water on the stigma can stimulate GO toxicity. Two sets of *C. avellana* CTRL and GO samples (n = 5–7) were rinsed in dH_2O. The first set (CTRL- or GO-PRE) was rinsed in 500 μL of dH_2O for 30 s and then let to dry out for 1.5 h in laboratory conditions (see above) before pollination. The second set (CTRL- or GO-POST) was first pollinated and then rinsed in dH_2O as previously described. All samples were maintained in a humid chamber overnight and then pollen adhesion and germination were assessed (see Section 2.7). Three samples per treatment prepared as described in Section 2.7 were then subjected to CLSM observations (see Section 2.5).

2.9. Statistical analysis

Statistical analysis was performed using the Dplyr software package in the R environment (R, version 3.6.3., February 29, 2020, The R foundation for statistical analysis) (Bunn, 2008). Significant differences in pollen detachment and pollen germination were assessed with generalized linear models (GLMs), assuming treatments as categorical predictors. Differences among treatments were assessed with the *post hoc* pairwise *t*-test using the Bonferroni adjusted method. Differences with Pr and p values <0.05 were considered statistically significant.

3. Results and discussion

In this work, we tested the effect of airborne GOs on the sexual reproduction of anemophilous plants by comparing untreated female flowers (CTRL) with flowers exposed to an atmosphere enriched in 0 or 3.7 ng m^{-3} of GO or PGO NPs (blank, GO and PGO samples, respectively; see Section 2.4). Nebulization of liquid GRMs dispersions with an airbrush is a common method for coating surfaces with GRMs (Pham et al., 2010; Ibrahim and Lin, 2018) but to the best of our knowledge it was never used before to treat aerial organs of plants. Additionally, it allowed to obtain a deposition of GO NPs in a dry state, a condition rarely applied but potentially relevant for anemophilous flowers which may be exposed to airborne GRMs.

3.1. Interception of airborne GO NPs by anemophilous stigmas and their effect on the stigmatic surface

The capability of anemophilous flowers to intercept airborne GO was tested in four seed plants differing in the morphology and chemistry (dry *vs.* wet) of their stigmatic surface (see Section 2.1), *i.e.* important characteristics for intercepting and retaining pollen (but also other PM) from air (Ackerman, 2000). Confocal laser scanning microscopy (CLSM) in reflectance mode revealed that all pristine stigmatic surfaces reflected a weak light when illuminated (Fig. 1). The light was also reflected from single spots on the stigmatic surfaces of blank and CTRL samples (Fig. 1a,c,e,h), purportedly caused by particles of unknown nature. In general, GO and PGO NPs were clearly distinguishable from the background signal by the more intense light reflected by their flat surfaces. GO NPs appeared evenly distributed on the stigmatic surfaces of exposed samples (Fig. 1b,d,f,i) and adhering to the walls of stigmatic cells or in few cases in between (Fig. 1g). Interestingly, an aggregate/flake was found regularly disposed almost on every stigmatic cell of the studied surfaces, indicating a non-random entrapment of NPs. Indeed, in anemophilous species, the interaction of air fluid dynamics with biological structures such as stigmatic papillae, trichomes, *etc.*, creates localized air turbulence that ensures the deposition of conspecific pollen grains on the stigma (Ackerman, 2000). The same mechanism could apply to airborne (GO) NPs.

The z-projection obtained by merging successive stacks (see Section 4.5) confirmed that the GO NPs (lateral dimension 0.5–30 μm) were neither internalized into the cytoplasm of the cells nor had penetrated in the underlying tissues of the pistils (Fig. 1g). This finding confirms previous observations on plant cells or tissues suggesting that the plant cell wall is an effective barrier toward flakes larger than 100 nm (24, 45): only very small flakes (40–60 nm) are rarely internalized or penetrate, and generally only when the cell has a thin wall (Zhao et al., 2015, 2017; Montagner et al., 2017).

Because CLSM images do not allow clear identification of stigmatic surface injury, SEM in environmental mode (ESEM) was used. ESEM observations confirmed the absence of GO NPs on CTRL (Fig. 2a,c,e,g) and blank samples. In GO-exposed samples, the integrity of the stigmatic surfaces was confirmed even when almost all stigmatic cells were in contact with one or more NPs (Fig. 2b,d,f,h). Signs of damage such as wilted papillae, crests or trichomes, or cytoplasmic leachates were never observed in all the species examined. These observations are consistent with those made on the dry stigma of entomophilous *C. pepo* exposed to dry GO and PGO NPs at higher doses than that here applied (Zanelli et al., 2022).

3.2. GO and PGO effect on the pollen-stigma system under dry and wet conditions

External adhesion of xenobiotics, such as GO or PGO NPs, to the stigmatic surface could affect pollen-stigma interaction (Candotto Carniel et al., 2018, 2020; Zanelli et al., 2021). Therefore, we simulated wind pollination and evaluated pollen adhesion and germination on the stigma of CTRL, blanks and treated samples according to Zanelli et al. (2020). Pollen adhesion in CTRL and blank samples was not significantly different in all the four species (Fig. 3a,c,e,g and Table S2) and pollen covered homogeneously about 3% of the stigmatic surface (SI-S2). Treatment with GO significantly decreased pollen adhesion with respect to CTRLs by 3.5 and 2-fold in *J. regia* and *Q. ilex*, respectively (Figs. 3a,c,e,g and Table S2), whereas PGO did not change pollen adhesion in all the four species. Although physical and chemical effects can alter pollen adhesion (Cox, 1988; Zhang et al., 2019; Zanelli et al., 2020), we can exclude the physical interposition of the flakes between pollen and stigma, as observed when GRMs were applied in high amounts (approx. 1 mg per stigma) to the stigma of *C. pepo* (Zanelli et al., 2020, 2021), because the coverage of flakes was homogeneous but low compared with the aforementioned studies (SI-S2). As for potential chemical interactions, the different compositions of GO and PGO could actually be the cause of the decrease in pollen adhesion observed in *J. regia* and *Q. ilex*. The elemental analysis of GO dispersions (100 μg mL^{-1}) before and after the purification step revealed that this treatment decreased the concentration of K, Mn and S from 328.6 ± 29.1, 592.8 ± 78.1 and 9167.0 ± 798.0 μg L^{-1} to 21.3 ± 2.5, 12.0 ± 8.4 and 594.0 ± 190.0 μg L^{-1}, respectively (GO *vs* PGO, Table S1). These elements derive from the strong acids and oxidants (mostly H_2SO_4 and $KMnO_4$) used to produce GO and are still present in the commercial batch, both in the dispersion H_2O and bound to the graphene matrix. The absence of effects in PGO-exposed samples and the similar effects observed on pollen adhesion caused by reactive substances possibly bound to airborne PM (Farmer, 1993; Yi et al., 2003; Zhang et al., 2019) further supports the hypothesis that the negative effects observed on pollen adhesion are caused by GO production residues. A reduced pollen adhesion lowers the density of pollen tubes growing through the stigmatic surface, and thus *de facto* lowers competition between pollen grains (Winsor et al., 1987; Hiscock and Allen, 2008). This may affect counterintuitively the success of the overall reproductive process, altering seed size and seedling vigor (Ter-Avanesian, 1978).

Pollen germination over the stigma surface was 93 ± 6, 67 ± 11%, 89 ± 4% and 89 ± 7% in CTRL flowers of *C. avellana*, *J. regia*, *Q. ilex* and *Z. mays*, respectively, and it did not differ in blank flowers. Unlike pollen adhesion, pollen germination on the stigma was never affected by the presence of GOs in any of the species tested (Fig. 3b,d,f,h and Table S3), as observed in *C. pepo* under similar conditions (Zanelli et al., 2022).

Differently, *in vitro* studies of pollen performance in response to GRMs showed that GO can affect germination and pollen tube elongation in

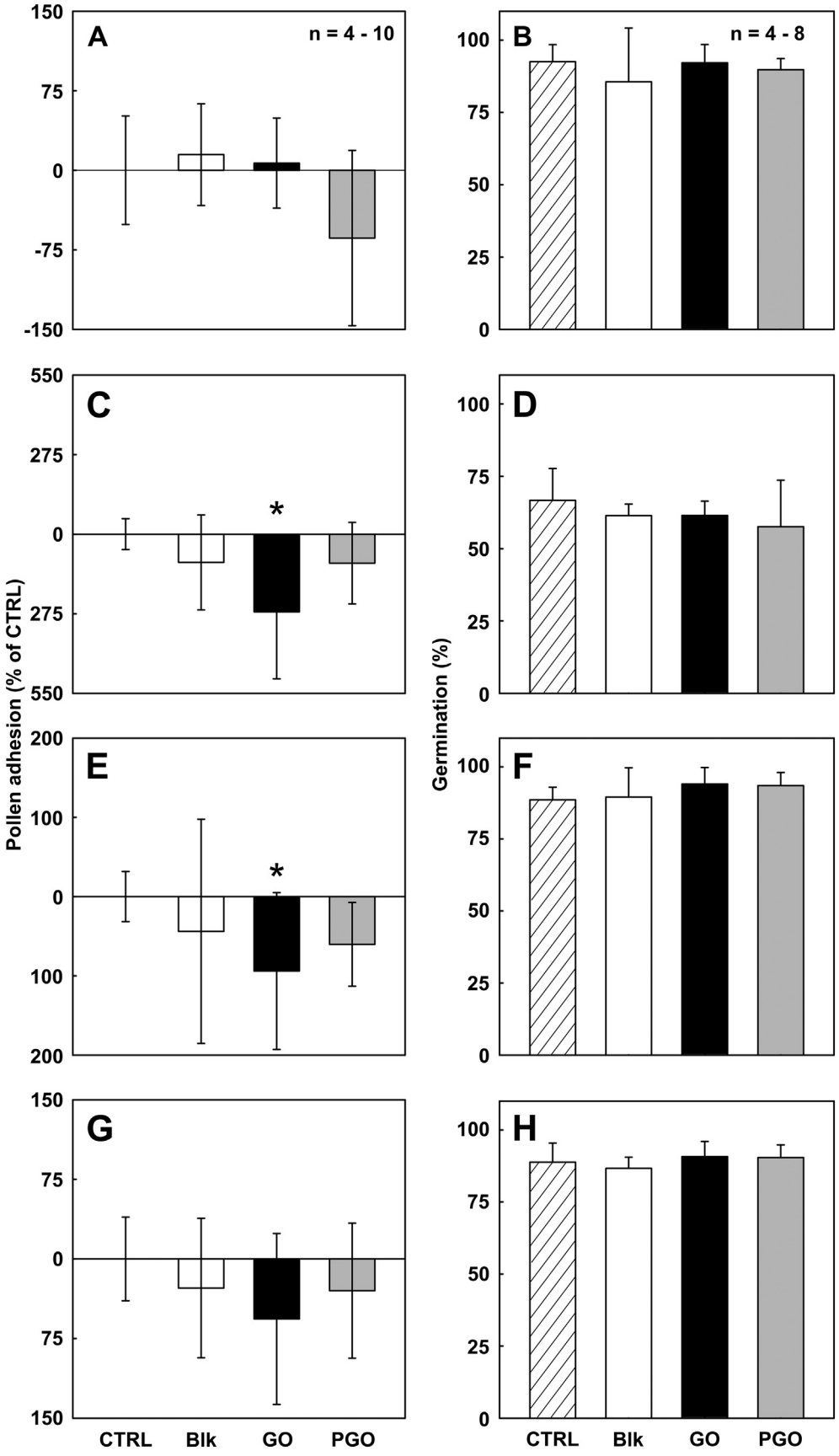

Fig. 3. Pollen-stigma interaction of *Corylus avellana* (A, B), *Juglans regia* (C, D), *Quercus ilex* (E, F), and *Zea mays* (G, H) flowers not exposed (CTRL) or after exposure to 0 (Blk) or 3.7 ng m^{-3} GO or purified-GO (PGO) and then pollinated (for more details, see Sections 2.4, 2.6, 2.8). Pollen adhesion (A, C, E, G) and pollen germination (B, D, F, H) on CTRL, Blk, GO and PGO-treated stigmas. Values are means ± s.d (n = 4–10); * = statistically different groups (GLM analysis *post-hoc t*-test; see Table S3).

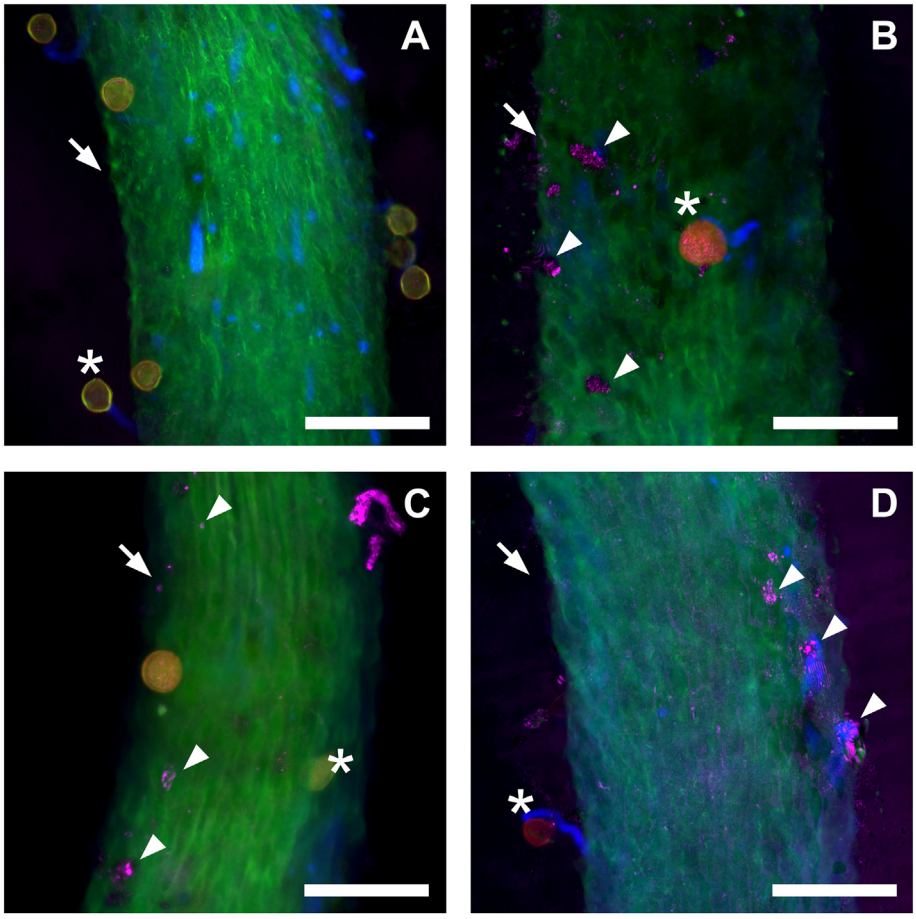

Fig. 4. Interaction of GO nanoparticles (NPs) with the pollen-stigma system of *Corylus avellana* in presence of a film of distilled water (dH_2O). Confocal laser scanning microscopy micrographs of the stigmatic surfaces not exposed (A) and after exposure (B) to GO and then pollinated, or after exposure to GO and then rinsed in dH_2O before (C) or after (D) pollination (for more details, see Sections 2.4, 2.5, 2.7). Green signal: autofluorescence of chlorophylls and pollen walls (weak); red signal: pollen grains autofluorescence; blue signal: aniline blue staining; pink signal: light reflected by GO sheets. Arrows = stigmatic surface; arrowheads = GO flakes; * = germinated pollen grains; bars = 200 μm.

C. avellana (Candotto Carniel et al., 2018). This is caused by the oxygen functional groups of GO (*e.g.*, carboxylic, epoxy, and oxydril groups), which alter H^+ and Ca^{2+} availability in the growth medium, thus affecting pollen homeostasis (Candotto Carniel et al., 2020). The results of Fig. 3 show that *in vivo* the negative effects caused by the acidic nature of GO are effectively counteracted by the local environment, most likely due to the buffering ability of the released sticky substances. Under natural conditions though, these substances could potentially be diluted by water films or droplets from fog, dew or rain, whereas GO NPs could deprotonate in the liquid environment and acidify the solution locally. To test this hypothesis, we focused on *C. avellana* because the pollen of this species showed deleterious *in vitro* effects when exposed to GO (Candotto Carniel et al., 2018, 2020). Therefore, *C. avellana* stigmas were wetted with dH_2O before (CTRL- and GO-PRE) and after (CTRL- and GO-POST) pollination. Wetting of GO-PRE and/or GO-POST samples partially removed the GO NPs from the stigmatic surface (Fig. 4b,c,d). Pollen adhesion was not affected whereas a tendency to decrease (c. – 33% on average) in pollen germination was observed only in GO-POST samples, even if this difference was not statistically significant ($Pr > 0.05$, GLM analysis; compare the GO-PRE and GO-POST treatments with the corresponding CTRLs, *i.e.*, CTRL-PRE and CTRL-POST, respectively: Fig. 5, Table S4). It can be concluded that the stigma of *C. avellana* can cope with the reactivity of GO by maintaining a favorable environment for pollen germination even under humid, dew-forming conditions, possibly also in this case due to a buffering capability of the stigmatic surface, whose nature remains unknown.

4. Conclusions

This study shows for the first time that: (*i*) anemophilous flowers can intercept airborne GO NPs at very low atmospheric concentrations and (*ii*) depending on the chemistry and structure of the exposed stigmatic surface, GO can affect pollen adhesion but not germination. Moreover, liquid water films possibly present on the stigmas of *C. avellana* did not promote GO toxic effects due to its acidic nature, suggesting that stigmas have an intrinsic buffering capability. Nonetheless, the long-lasting receptivity of some anemophilous species such as *C. avellana* could favor the accumulation of GO NPs on the stigma, possibly resulting in more severe effects than those observed in this study. In contrast to GO, airborne PGO never affected the interaction between pollen and stigma in the species tested, emphasizing that the production residues possibly present in GO are the main cause of the adverse effects observed.

CRediT authorship contribution statement

Author contributions: **Davide Zanelli**: Conceptualization, Data curation, Formal analysis, Investigation, Methodology, Resources, Validation, Visualization, Writing - original draft, Writing - review & editing; **Fabio Candotto Carniel**: Conceptualization, Formal analysis, Investigation, Methodology, Project administration, Resources, Supervision, Validation, Writing - original draft, Writing - review & editing; **Lorenzo Fortuna**: Conceptualization, Data curation, Formal analysis, Investigation,

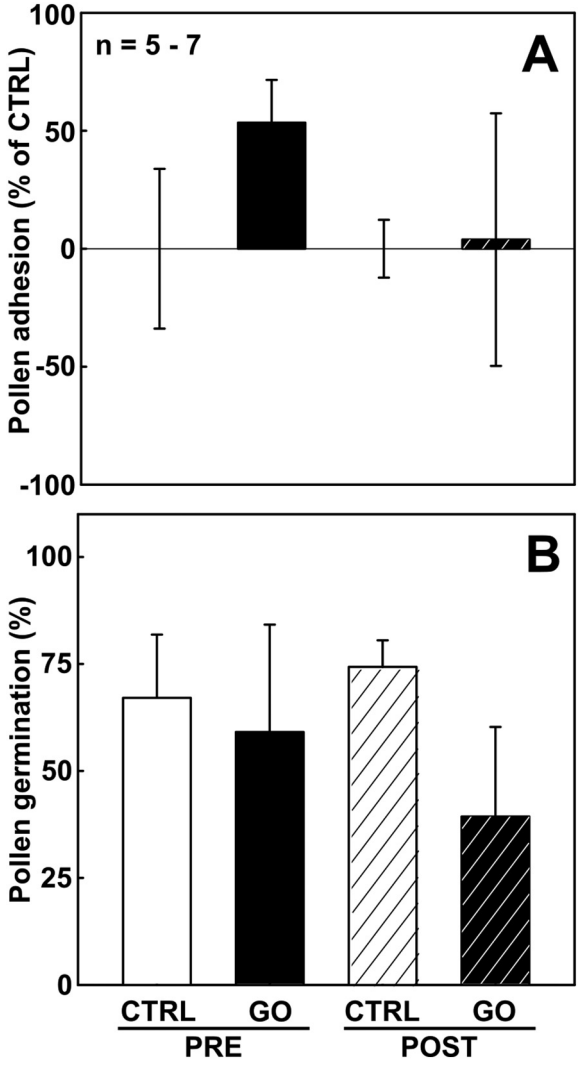

Fig. 5. Pollen-stigma interaction of *Corylus avellana* flowers not exposed (CTRL) or after exposure to GO and then rinsed in dH_2O before (PRE) or after (POST) being subjected to pollination (for more details, see Sections 2.4, 2.6–2.8). (E) Pollen adhesion and (F) germination on CTRL-PRE, GO-PRE, CTRL-POST and GO-POST-treated stigmas. Values are means ± s.d. (n = 5–7).

Methodology, Validation, Writing - original draft; **Elena Pavoni**: Investigation; **Viviana Jehová González**: Investigation; **Ester Vázquez**: Funding acquisition, Resources, Supervision; **Maurizio Prato**: Funding acquisition, Resources; **Mauro Tretiach**: Conceptualization, Funding acquisition, Methodology, Project administration, Resources, Supervision, Writing - original draft, Writing - review & editing.

Declaration of competing interest

The authors declare that they have no known competing financial interests or personal relationships that could have appeared to influence the work reported in this paper.

Acknowledgments

This work was supported by the Graphene Flagship Core 2 and Core 3 grant agreement (no. 785219 and 881603, respectively), the University of Trieste DOTTAMBIENTEVITA34-18. The authors would like to thank Prof. Fabio Gaiotti (University of Trieste) for the advice and discussion on the developing of the exposure chamber; Giovanni and Gregorio Motta (Desio, Italy) for the assistance to build up the exposure chamber; Emanuele and Marco Loro (Latisana, Italy) for suppling hazelnut plants; Nicolò Panciera (Pordenone, Italy) and Giuliano Cicuttin (Latisana, Italy) for the support with walnut and corn sampling, respectively; Dr. Gianluca Turco and Dr. Davide Porelli (University of Trieste) for the help in ESEM analysis.

Appendix A. Supplementary data

Supplementary data to this article can be found online at https://doi.org/10.1016/j.scitotenv.2022.154625.

References

Ackerman, J.D., 2000. Abiotic pollen and pollination: ecological, functional, and evolutionary perspectives. Plant Syst. Evol. 222, 167–185. https://doi.org/10.1007/BF00984101.

Ali-Boucetta, H., Bitounis, D., Raveendran-Nair, R., Servant, A., Van den Bossche, J., Kostarelos, K., 2013. Purified graphene oxide dispersions lack in vitro cytotoxicity and in vivo pathogenicity. Adv. Healthc. Mater. 2, 433–441. https://doi.org/10.1002/adhm.201200248.

Andelkovic, I.B., Kabiri, S., Tavakkoli, E., Kirby, J.K., McLaughlin, M.J., Losic, D., 2018. Graphene oxide-Fe(III) composite containing phosphate – a novel slow release fertilizer for improved agriculture management. J. Clean. Prod. 185, 97–104. https://doi.org/10.1016/j.jclepro.2018.03.050.

Banchi, E., Candotto Carniel, F., Montagner, A., Bosi, S., Bramini, M., Crosera, M., León, V., Martín, C., Pallavicini, A., Vázquez, E., Prato, M., Tretiach, M., 2019. Graphene-based materials do not impair physiology, gene expression and growth dynamics of the aeroterrestrial microalga Trebouxia gelatinosa. Nanotoxicology 13, 492–509. https://doi.org/10.1080/17435390.2019.1570371.

Boccuni, F., Ferrante, R., Tombolini, F., Natale, C., Gordiani, A., Sabella, S., Iavicoli, S., 2020. Occupational exposure to graphene and silica nanoparticles. Part I: workplace measurements and samplings. Nanotoxicology 14, 1280–1300. https://doi.org/10.1080/17435390.2020.1834634.

Bonaccorso, F., Colombo, L., Yu, G., Stoller, M., Tozzini, V., Ferrari, A.C., Ruoff, R.S., Pellegrini, V., 2015. Graphene, related two-dimensional crystals, and hybrid systems for energy conversion and storage. Science 347, 1246501. https://doi.org/10.1126/science.1246501.

Bramini, M., Sacchetti, S., Armirotti, A., Rocchi, A., Vázquez, E., Castellanos, V.L., Bandiera, T., Cesca, F., Benfenati, F., 2016. Graphene oxide nanosheets disrupt lipid composition, Ca2+ homeostasis, and synaptic transmission in primary cortical neurons. ACS Nano 10, 7154–7171. https://doi.org/10.1021/ACSNANO.6B03438.

Bunn, A.G., 2008. A dendrochronology program library in R (dplR). Dendrochronologia 26, 115–124. https://doi.org/10.1016/j.dendro.2008.01.002.

Candotto Carniel, F., Gorelli, D., Flahaut, E., Fortuna, L., Del Casino, C., Cai, G., Nepi, M., Prato, M., Tretiach, M., 2018. Graphene oxide impairs the pollen performance of Nicotiana tabacum and Corylus avellana suggesting potential negative effects on the sexual reproduction of seed plants. Environ. Sci. Nano 5, 1608–1617. https://doi.org/10.1039/C8EN00052B.

Candotto Carniel, F., Fortuna, L., Nepi, M., Cai, G., Del Casino, C., Adami, G., Bramini, M., Bosi, S., Flahaut, E., Martín, C., Vázquez, E., Prato, M., Tretiach, M., 2020. Beyond graphene oxide acidity: novel insights into graphene related materials effects on the sexual reproduction of seed plants. J. Hazard. Mater. 393, 122380. https://doi.org/10.1016/j.jhazmat.2020.122380.

Candotto Carniel, F., Fortuna, L., Zanelli, D., Garrido, M., Vázquez, E., González, V.J., Prato, M., Tretiach, M., 2021. Graphene environmental biodegradation: wood degrading and saprotrophic fungi oxidize few-layer graphene. J. Hazard. Mater. 414, 125553. https://doi.org/10.1016/j.jhazmat.2021.125553.

Ciampolini, F., Cresti, M., 1998. The structure and cytochemistry of the stigma-style complex of Corylus avellana L. 'Tonda gentile delle langhe' (Corylaceae). Ann. Bot. 81, 513–518. https://doi.org/10.1006/anbo.1998.0586.

Cox, R.M., 1988. Sensitivity of forest plant reproduction to long-range transported air pollutants: the effects of wet deposited acidity and copper on reproduction of Populus tremuloides. New Phytol. 110, 33–38. https://doi.org/10.1111/j.1469-8137.1988.tb00234.x.

Dupuis, I., Dumas, C., 1990. Biochemical markers of female receptivity in maize (Zea mays L.) assessed using in vitro fertilization. Plant Sci. 70, 11–19. https://doi.org/10.1016/0168-9452(90)90026-K.

Fadeel, B., Bussy, C., Merino, S., Vázquez, E., Flahaut, E., Mouchet, F., Evariste, L., Gauthier, L., Koivisto, A.J., Vogel, U., Martín, C., Delogu, L.G., Buerki-Thurnherr, T., Wick, P., Beloin-Saint-Pierre, D., Hischier, R., Pelin, M., Candotto Carniel, F., Tretiach, M., Cesca, F., Benfenati, F., Scaini, D., Ballerini, L., Kostarelos, K., Prato, M., Bianco, A., 2018. Safety assessment of graphene-based materials: focus on human health and the environment. ACS Nano 12, 10582–10620. https://doi.org/10.1021/acsnano.8b04758.

Farmer, A.M., 1993. The effects of dust on vegetation – a review. Environ. Pollut. 79, 63–75. https://doi.org/10.1016/0269-7491(93)90179-R.

Fusco, L., Garrido, M., Martín, C., Sosa, S., Ponti, C., Centeno, A., Alonso, B., Zurutuza, A., Vázquez, E., Tubaro, A., Prato, M., Pelin, M., 2020. Skin irritation potential of graphene-based materials using a non-animal test. Nanoscale 12, 610–622. https://doi.org/10.1039/c9nr06815e.

Gao, H., He, W., Yu, R., Hammer, T., Xu, G., Wang, J., 2020. Aerodynamic property and filtration evaluation of airborne graphene nanoplatelets with plate-like shape and folded structure. Sep. Purif. Technol. 251, 117293. https://doi.org/10.1016/J.SEPPUR.2020.117293.

Germain, E., 1994. The reproduction of hazelnut (Corylus avellana L.): a review. Acta Hortic. https://doi.org/10.17660/actahortic.1994.351.19.
Gil-Pelegrín, E., Javier, J., Domingo, P.-P., Editors, S.-K., 2017. Oaks physiological ecology. Exploring the functional diversity of genus Quercus L. Tree Physiology. Springer International Publishing, Cham https://doi.org/10.1007/978-3-319-69099-5.
Heslop-Harrison, Y., 1977. The receptive surface of the angiosperm stigma. Ann. Bot. 41, 1233–1258. https://doi.org/10.1093/oxfordjournals.aob.a085414.
Heslop-Harrison, J., Heslop-Harrison, Y., 1970. Evaluation of pollen viability by enzymatically induced fluorescence; intracellular hydrolysis of fluorescein diacetate. Stain. Technol. 45, 115–120. https://doi.org/10.3109/10520297009085351.
Heslop-Harrison, Y., Reger, B.J., Heslop-Harrison, J.S., 1984. The pollen-stigma interaction in the grasses. 5. Tissue organisation and cytochemistry of the stigma ("silk") of zea mays L. Acta Bot. Neerl. 33, 81–99. https://doi.org/10.1111/j.1438-8677.1984.tb01774.x.
Hiscock, S.J., Allen, A.M., 2008. Diverse cell signalling pathways regulate pollen-stigma interactions: the search for consensus. New Phytol. 179, 286–317. https://doi.org/10.1111/j.1469-8137.2008.02457.x.
Ibrahim, A.F.M., Lin, Y.S., 2018. Synthesis of graphene oxide membranes on polyester substrate by spray coating for gas separation. Chem. Eng. Sci. 190, 312–319. https://doi.org/10.1016/J.CES.2018.06.031.
Ivar Do Sul, J.A., Costa, M.F., 2014. The present and future of microplastic pollution in the marine environment. Environ. Pollut. 185, 352–364. https://doi.org/10.1016/J.ENVPOL.2013.10.036.
Janković, S., Stanković, J., Janković, D., Milatović, D., 2021. Morphology and morphogenesis of female reproductive organs in some walnut (Juglans regia L.) genotypes. Sci. Hortic. 289, 110471. https://doi.org/10.1016/J.SCIENTA.2021.110471.
Jones, M.D., Newell, L.C., 1948. Longevity of pollen and stigmas of grasses: buffalo-grass, Buchloe dactyloides (Nutt.) Engelm., and corn, Zea mays L. Agron. J. 40, 195–204. https://doi.org/10.2134/agronj1948.00021962004000030001x.
Joshi, K., Mazumder, B., Chattopadhyay, P., Bora, N.S., Goyary, D., Karmakar, S., 2019. Graphene family of nanomaterials: reviewing advanced applications in drug delivery and medicine. Curr. Drug Deliv. 16, 195–214. https://doi.org/10.2174/1567201815666181031162208.
Krueger, W.H., 2000. Pollination of english walnuts: practices and problems. HortTechnology 10, 127–130. https://doi.org/10.21273/HORTTECH.10.1.127.
Liu, J., Zhao, Q., Zhang, X., 2017. Structure and slow release property of chlorpyrifos/graphene oxide-ZnAl-layered double hydroxide composite. Appl. Clay Sci. 145, 44–52. https://doi.org/10.1016/j.clay.2017.05.023.
Lovén, K., Franzén, S.M., Isaxon, C., Messing, M.E., Martinsson, J., Gudmundsson, A., Pagels, J., Hedmer, M., Lovén, K., Franzén, S.M., Isaxon, C., Messing, M.E., Gudmundsson, A., Pagels, J., Hedmer, M., 2021. Emissions and exposures of graphene nanomaterials, titanium dioxide nanofibers, and nanoparticles during down-stream industrial handling. J. Expo. Sci. Environ. Epidemiol. 31, 736–752. https://doi.org/10.1038/s41370-020-0241-3.
Mertens, R., 2021. In: Mertens, Ron (Ed.), The Graphene Handbook, 2021.
Miniero, R., Iamiceli, A.L., De Felip, E., 2015. Persistent organic pollutants. Reference Module in Earth Systems and Environmental Sciences. Elsevier Reference Collection https://doi.org/10.1016/B978-0-12-409548-9.09496-3.
Miraftab, R., Xiao, H., 2019. Feasibility and potential of graphene and its hybrids with cellulose as drug carriers : a commentary. J. Bioresour. Bioprod. 4, 200–201. https://doi.org/10.12162/jbb.v4i4.013.
Mitrano, D.M., Wick, P., Nowack, B., 2021. Placing nanoplastics in the context of global plastic pollution. Nat. Nanotechnol. 16, 491–500. https://doi.org/10.1038/s41565-021-00888-2.
Montagner, A., Bosi, S., Tenori, E., Bidussi, M., Alshatwi, A.A., Tretiach, M., Prato, M., Syrgiannis, Z., 2017. Ecotoxicological effects of graphene-based materials. 2D Mater. 4, 012001. https://doi.org/10.1088/2053-1583/4/1/012001.
Nepi, M., Pacini, E., 1993. Pollination, pollen viability and pistil receptivity in Cucurbita pepo. Ann. Bot. 72, 527–536. https://doi.org/10.1006/anbo.1993.1141.
Nepi, M., Franchi, G.G., Pacini, E., 2001. Pollen hydration status at dispersal: cytophysiological features and strategies. Protoplasma 216, 171–180. https://doi.org/10.1007/BF02673869.
Netkueakul, W., Korejwo, D., Hammer, T., Chortarea, S., Rupper, P., Braun, O., Calame, M., Rothen-Rutishauser, B., Buerki-Thurnherr, T., Wick, P., Wang, J., 2020. Release of graphene-related materials from epoxy-based composites: characterization, quantification and hazard assessment in vitro. Nanoscale 12, 10703–10722. https://doi.org/10.1039/C9NR10245K.
Nine, M.J., Cole, M.A., Tran, D.N.H., Losic, D., 2015. Graphene: a multipurpose material for protective coatings. J. Mater. Chem. A 12580–12602. https://doi.org/10.1039/C5TA01010A.
Novoselov, K.S., Geim, A.K., Morozov, S.V., Jiang, D., Zhang, Y., Dubonos, S.V., Grigorieva, I.V., Firsov, A.A., 2004. Electric field effect in atomically thin carbon films. Science 306, 666–669. https://doi.org/10.1126/science.1102896.
Novoselov, K.S., Fal'Ko, V.I., Colombo, L., Gellert, P.R., Schwab, M.G., Kim, K., 2012. A roadmap for graphene. Nature 490, 192–200. https://doi.org/10.1038/nature11458.
Pham, V.H., Cuong, T.V., Hur, S.H., Shin, E.W., Kim, J.S., Chung, J.S., Kim, E.J., 2010. Fast and simple fabrication of a large transparent chemically-converted graphene film by spray-coating. Carbon 48, 1945–1951. https://doi.org/10.1016/J.CARBON.2010.01.062.
Shamsaei, E., de Souza, F.B., Yao, X., Benhelal, E., Akbari, A., Duan, W., 2018. Graphene-based nanosheets for stronger and more durable concrete: a review. Constr. Build. Mater. 183, 642–660. https://doi.org/10.1016/J.CONBUILDMAT.2018.06.201.
Sun, T.Y., Gottschalk, F., Hungerbühler, K., Nowack, B., 2014. Comprehensive probabilistic modelling of environmental emissions of engineered nanomaterials. Environ. Pollut. 185, 69–76. https://doi.org/10.1016/J.ENVPOL.2013.10.004.
Sun, T.Y., Bornhöft, N.A., Hungerbühler, K., Nowack, B., 2016. Dynamic probabilistic modeling of environmental emissions of engineered nanomaterials. Environ. Sci. Technol. Technol. 50, 4701–4711. https://doi.org/10.1021/acs.est.5b05828.
Ter-Avanesian, D.V., 1978. The effect of varying the number of pollen grains used in fertilization. Theor. Appl. Genet. 52, 77–79. https://doi.org/10.1007/BF00281320.
Tombolini, F., Boccuni, F., Ferrante, R., Natale, C., Marasco, L., Mantero, E., Del Rio Castillo, A.E., Leoncino, L., Pellegrini, V., Sabella, S., Iavicoli, S., 2021. An integrated and multi-technique approach to characterize airborne graphene flakes in the workplace during production phases. Nanoscale 13, 3841–3852. https://doi.org/10.1039/D0NR07114E.
Wang, X., Xie, H., Wang, Z., He, K., 2019. Graphene oxide as a pesticide delivery vector for enhancing acaricidal activity against spider mites. Colloids Surf. B Biointerfaces 173, 632–638. https://doi.org/10.1016/j.colsurfb.2018.10.010.
Weinbruch, S., Benker, N., Kandler, K., Schütze, K., Kling, K., Berlinger, B., Thomassen, Y., Drotikova, T., Kallenborn, R., 2018. Source identification of individual soot agglomerates in Arctic air by transmission electron microscopy. Atmos. Environ. 172, 47–54. https://doi.org/10.1016/j.atmosenv.2017.10.033.
Winsor, J.A., Davis, L.E., Stephenson, A.G., 1987. The relationship between pollen load and fruit maturation and the effect of pollen load on offspring vigor in Cucurbita pepo. Am. Nat. 129, 643–656. https://doi.org/10.1086/284664.
Yi, W., Law, S.E., Wetzstein, H.Y., 2003. Fungicide sprays can injure the stigmatic surface during receptivity in almond flowers. Ann. Bot. 91, 335–341. https://doi.org/10.1093/aob/mcg019.
Zanelli, D., Candotto Carniel, F., Garrido, M., Fortuna, L., Nepi, M., Cai, G., Del Casino, C., Vázquez, E., Prato, M., Tretiach, M., 2020. Effects of few-layer graphene on the sexual reproduction of seed plants: an in vivo study with Cucurbita pepo L. Nanomaterials 10, 1877. https://doi.org/10.3390/nano10091877.
Zanelli, D., Candotto Carniel, F., Fortuna, L., Pavoni, E., González, V.J., Vázquez, E., Prato, M., Tretiach, M., 2022. From flower to seed: how simulated dry depositions of airborne graphene oxides interact with the sexual reproduction of a model plant. Environ. Sci. Nano under review.
Zanelli, D., Candotto Carniel, F., Tretiach, M., 2021. The interaction of graphene oxide with the pollen − stigma system : in vivo effects on the sexual reproduction of Cucurbita pepo L. Appl. Sci. 11, 6150. https://doi.org/10.3390/app11136150.
Zhang, L., Beede, R.H., Banuelos, G., Wallis, C.M., Ferguson, L., 2019. Dust interferes with pollen–stigma interaction and fruit set in pistachio Pistacia vera cv. Kerman. HortScience 54, 1967–1971. https://doi.org/10.21273/HORTSCI14330-19.
Zhao, S., Wang, Q., Zhao, Y., Rui, Q., Wang, D., 2015. Toxicity and translocation of graphene oxide in Arabidopsis thaliana. Environ. Toxicol. Pharmacol. 39, 145–156. https://doi.org/10.1016/j.etap.2014.11.014.
Zhao, J., Cao, X., Wang, Z., Dai, Y., Xing, B., 2017. Mechanistic understanding toward the toxicity of graphene-family materials to freshwater algae. Water Res. 111, 18–27. https://doi.org/10.1016/j.watres.2016.12.037.